Hindawi
International Journal of Antennas and Propagation
Volume 2022, Article ID 7935581, 11 pages
https://doi.org/10.1155/2022/7935581

Research Article

A Novel Universal Applicability Design Method for Low Cross-Polarization Terahertz Tri-Reflector CATR

Zhi Li,[1] Yuan Yao ,[1] Tianyang Chen,[1] Liang Zhang,[1] Junsheng Yu,[1] and Xiaodong Chen[2]

[1]*The School of Electronic Engineering, Beijing University of Posts and Telecommunications, Beijing 100876, China*
[2]*The School of Electronic Engineering and Computer Science, Queen Mary University of London, London E1 4NS, UK*

Correspondence should be addressed to Yuan Yao; yaoy@bupt.edu.cn

Received 29 January 2022; Revised 5 November 2022; Accepted 7 November 2022; Published 15 November 2022

Academic Editor: Ravi Gangwar

In this paper, a novel design approach with universal applicability is proposed for realizing a low cross-polarized terahertz tri-reflector compact antenna test range (CATR). This approach not only enables the radiation direction of the feed relative to the main reflector to be designed arbitrarily but also enables the designed CATR systems corresponding to different feed rotation angles while still maintaining a low cross-polarization. By using the beam mode analysis method and cross-polarization elimination conditions, the geometric configurations of the tri-reflector CATR can be designed for feeds in any different rotation angles, and then according to the kinematic and dynamic ray-tracing method with frequency independence in geometric optics, shaped subreflectors can also be synthesized. Through the above design procedure, four tri-reflector CATRs corresponding to four different feed rotation angles have been achieved, respectively. Numerical simulation results show that the cross-polarizations of four tri-reflector CATRs are all less than −38 dB and the peak-to-peak amplitude (phase) ripples of the quiet zone (QZ) are all within 1 dB (10°) in the frequency range of 100–500 GHz. This demonstrates the effectiveness and universal applicability of the proposed design method in realizing the design of low cross-polarization and good QZ performance for tri-reflector CATRs with different feed rotation angles.

1. Introduction

With the widespread application of millimeter wave and terahertz technology in radio astronomy, remote sensing, satellite detection, and other fields [1, 2], the demand for accurate measurement of millimeter wave and terahertz electrically large aperture antennas is becoming more and more urgent. At present, there are mainly three test methods for antenna measurement: one is to directly measure the far-field [3], the other is the near-field or far-field conversion [4, 5], and the third is the compact antenna test range (CATR) measurement [6–9]. The conventional far-field method requires a long distance between the large aperture antenna under test and the radiating unit in millimeter wave and terahertz frequency bands. At the same time, the strong absorption of the atmosphere and background radiation will also make it challenging to take a measurement in the far field. In the near-field method, the field measurements at high frequency suffer many difficulties, including scanning inaccuracy, phase errors, long scanning time, and so forth. However, the CATR can better overcome the above problems. A CATR can collimate the field distribution from a feed to produce a pseudoplane wave in a relatively short distance which is the only feasible approach to measure large aperture antennas in the bands of millimeter wave and terahertz.

Since CATR can generate a regional pseudoplane wave, usually referred to as a quiet zone (QZ), the performance of the QZ, which includes the ripples of amplitude and phase, reflector aperture usage efficiency, and cross-polarization, can be used as an important basis for evaluating CATR. At present, there are several ways to build a reflector CATR [10–13]. The most common reflector type CATR is the single offset parabolic reflector CATR. For example, Professor C. G. Parini et al. built an offset single reflector CATR in QMUL, the upper limit of working frequency is 100 GHz, aperture length is 3 m, and QZ diameter is 1 m [14]. However, the drawback of this single reflector CATR is often referred to as its low QZ usage, typically 30%. In order to further reduce the amplitude and phase ripple and improve the aperture usage, many methods have been used by suppressing the edge diffractions of the reflector, such as the common reflector edge treatment method including serrations and blended rolled edges [15–17]. Moreover, the method of tapering the illumination amplitude near the reflector edges can be accomplished with a high-gain feed or an array feed design [18, 19]. These methods can make the aperture usage reach about 50%. However, the single offset fed reflector CATR suffers from a relatively high cross-polarization level due to its asymmetric structure in the offset plane. Although matched feed, shaped feed, and other methods can be used to improve cross-polarization by sacrificing bandwidth [20–22], performance improvement is still limited. There also exists a dual-reflector CATR; for example, Steiner et al. built the CCR75/60 dual-reflector CATR in Astrium, which can provide about 60% QZ usage [23, 24]. However, the size of the subreflector of the dual-reflector CATR is almost as large as that of the main reflector, which greatly increases the construction cost. At the same time, with the increase in frequency, the processing precision of large-size mirrors is also facing great challenges. To overcome the above shortcomings, a tri-reflector configuration has to be employed. For example, Yu et al. have designed a tri-reflector CATR with a parabolic main mirror diameter of 3 m, which can provide 70% of QZ usage and cross-polarization of about −40 dB in a working frequency of about 300 GHz [25, 26]. However, this CATR design method has certain limitations because it requires that the radiation direction of the feed must be consistent with the symmetry axis of the parabolic main reflector, and the structural form of the CATR is relatively single and fixed, especially the rotation angle of the feed cannot be flexibly designed according to the actual construction requirements. In addition, the principle of achieving low cross-polarization performance for the CATR designed by this method is still unclear and lacks certain theoretical support.

In order to improve the flexibility of the structural design of the tri-reflector CATR system and to meet the requirements for different building layouts of the CATR system under various environmental conditions with limited space size, a novel universal applicability tri-reflector CATR design method is proposed in this paper. This method has no restrictions on the structural form design of the tri-reflector CATR, especially on the radiation direction of the feed relative to the main reflector; that is, when using this design method and process, no matter how the feed's rotation angle changes, we can always design a tri-reflector CATR with high QZ usage and low cross-polarization performance. Table 1 lists the major performance between the proposed tri-reflector CATR system and the reported CATR systems. It can be seen from the table that the proposed tri-reflector CATR not only has higher QZ usage and lower cross-polarization, but also the size of the subreflector is much smaller than that of the main reflector, and more importantly, the feed's rotation angle of the system can be designed to any angle. Since the proposed design method is based on the beam mode analysis and cross-polarization elimination theory [27, 28], it has a sufficient theoretical basis. Therefore, this method can also provide theoretical and principle support for reasonably explaining why the tri-reflector CATR can achieve the characteristic of low cross-polarization. The main design process of this method is as follows: firstly, according to the beam mode analysis and cross-polarization elimination conditions in Section 2.1, the specific geometric configuration form with low cross-polarization characteristics of the tri-reflector CATR corresponding to different feed rotation angles can be analyzed and determined as shown in Figure 1. Moreover, the value of the structural parameter variables and the coordinate value of the central point in each reflector of the designed tri-reflector CATR system corresponding to any feed rotation angle can also be numerically calculated following the calculation steps of the coordinates value of the central point in the second paragraph of Section 2.2. Secondly, by using the kinematic and dynamic ray-tracing method in geometric optics [29], we can use the ray emitted by the feed source to illuminate the central point position of subreflector 1, subreflector 2, and the main reflector in turn and take them as the initial optic path, and then we adopt the surface reconstruction technology to construct two shaped subreflectors, which is described in detail in Section 2.2. Finally, the performance of the entire tri-reflector CATR system should be simulated in Section 3, and all the structural parameter variables of the system should be properly fine-tuned according to the simulation results to further optimize and complete the design of the low cross-polarization CATR system.

2. Universal Applicability Design of Tri-Reflector CATR

2.1. Cross-Polarization Elimination Conditions and Geometry. Figure 2(a) shows the schematic diagram of a tri-reflector CATR system designed using the proposed universal applicability design method. The tri-reflector CATR system is composed of a feed, two shaped subreflectors, and a parabolic main reflector with an aperture length of 3 m.

Since the geometric position of each reflector in the tri-reflector CATR system has a significant impact on the cross-polarization of the CATR system, thus determining the overall structure configuration form of the system and the coordinate of the central point in each reflector is particularly important for the design of a low cross-polarization system. Here, we have adopted the beam mode analysis method and cross-polarization elimination conditions [27] for system configuration design and coordinate calculation. For the beam mode analysis method, the focal lengths f_1, f_2, and f_3 of subreflector 1, subreflector 2, and the main reflector in the tri-reflector CATR system which are shown in Figure 2(a) are defined by (1), and the specific description is shown in Figure 2(b) as follows:

Table 1: Comparison between the proposed tri-reflector CATR system and the reported CATR systems.

References	Upper-frequency limit (GHz)	QZ usage (%)	QZ diameter (m)	Size of subreflectors (m)	Cross-polar (dB)	Feed rotation angle
[15]	300	42	0.25		−20	
[16]	110	50	0.6		−25	
[17]	100	50	0.15		−30	
[23]	200	66	5	5.6	−36	
[24]	200	70	6	6.1	−36	
Proposed	500	70	2.1	0.23 and 0.17	−38	Arbitrary

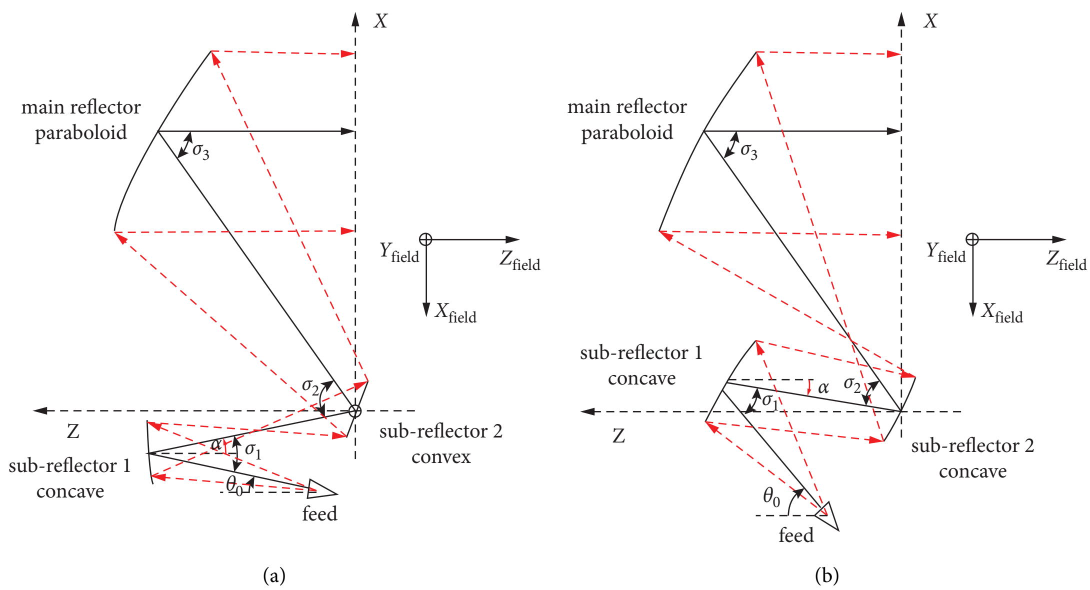

Figure 1: Specific configuration forms of tri-reflector CATR with low cross-polarization characteristics. (a) When $\alpha > 0$ and (b) when $\alpha < 0$.

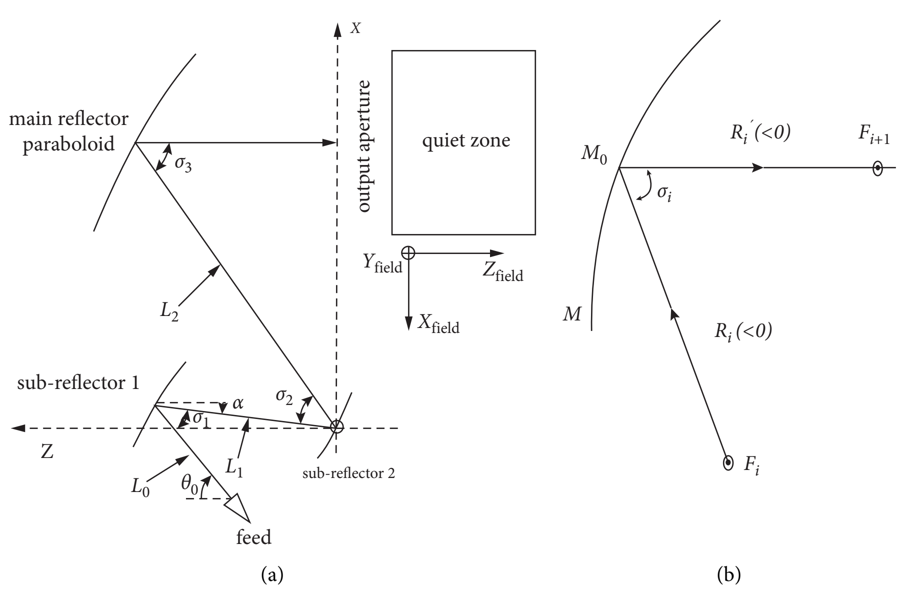

Figure 2: (a) Schematic diagram of geometric structure and design parameters of a tri-reflector CATR. (b) Definition of focal length in each reflector.

$$\begin{cases} \dfrac{1}{f_1} = \dfrac{1}{R_1} - \dfrac{1}{R_1'}, \\ \dfrac{1}{f_2} = \dfrac{1}{R_2} - \dfrac{1}{R_2'}, \\ \dfrac{1}{f_3} = \dfrac{1}{R_3} - \dfrac{1}{R_3'}, \end{cases} \quad (1)$$

where R_i and R_i' are the distances from the incident side focal point F_i and the reflection side focal point F_{i+1} to the intersection M_0 of the central ray and the reflector surface M.

To make the CATR system achieve low cross-polarization, the design should meet the cross-polarization elimination condition derived in [27], which is simplified as follows:

$$\begin{cases} f_1 = f_3 \dfrac{L_1 \tan(\sigma_1/2)}{L_2 \tan(\sigma_3/2)}, \\ f_2 = -\dfrac{f_3 \tan(\sigma_2/2)/L_2 \tan(\sigma_3/2) - 1}{1/L_1 + 1/L_2}, \\ R_3' = \infty, \end{cases} \quad (2)$$

where L_i represents the length of the ray in each section, R_3' represents the distance of the focus at infinity, σ_i represents the angle between the incident and reflected central rays, α represents the angle between the central ray of the second segment and the z-axis, α is positive in the counterclockwise direction, and θ_0 represents the angle between the direction of the central axis of the feed and the horizontal direction, which is denoted as the feed rotation angle in this paper, and all these variables are shown in Figure 2(a).

It can be seen from Figure 2(a) that when the angle variable θ_0 changes, the configuration form of the CATR system structure will also change accordingly. In order to develop a tri-reflector CATR system with low cross-polarization characteristics in any different feed rotation angles, first, we need to discuss the value relationship and range between relevant parameter variables in the above-mentioned cross-polarization elimination conditions. When the angle variable θ_0 is from the range of 0° to 90°, according to the definition and principle derivation in [27], we can know that subreflector 1 is concave if the main reflector is facing downward, that is, $f_1 > 0$, $f_3 > 0$, and the specific configuration forms of the system structure with low cross-polarization characteristics in Figure 2(a) can be divided into the following two kinds of different situations:

(1) When $\alpha > 0$, $\sigma_2 > \sigma_3$, $f_3 > L_2$, then $f_2 < 0$, that is, subreflector 2 is convex, and the tri-reflector CATR system structure can be obtained as shown in Figure 1(a)

(2) When $\alpha < 0$, $\sigma_2 < \sigma_3$, $f_3 < L_2$, then $f_2 > 0$, that is, subreflector 2 is concave, and the tri-reflector CATR system structure can be obtained as shown in Figure 1(b)

2.2. Design and Synthesis of Tri-Reflector CATR. According to the two specific structural configurations of the system and the value relationship between relevant parameter variables obtained in Section 2.1, by using the kinematic and dynamic ray-tracing method to shape the subreflectors [29], we can design a low-cross polarization tri-reflector CATR system regardless of the feed in any rotation angle.

However, the solution of the value of the central point coordinates in each reflector is the key to the whole shape design procedure. Here, the global coordinate XYZ is assumed to have its origin at the center of subreflector 2. To obtain the value of the central point coordinates in each reflector, firstly, the simultaneous equations, which are established by formulas (1) and (2) that satisfy the cross-polarization elimination conditions, should be programmed in MATLAB numerical calculation software together with the objective function, which is used to represent the cross-polarization of the CATR system. Then, we can assume that the parameter variables θ_0 and L_0 to be any desired constant values, such as $\theta_0 = 0°$, 30°, 60°, or 90°, $L_0 = 0.6$ m, and substitute them into the above-mentioned simultaneous equations. At the same time, we should optimize the value of the objective function by sweeping the parameter variables L_1, R_3, σ_2, and α within the range of values discussed in Section 2.1 with MATLAB numerical calculation software. Finally, we can select a set of variable values corresponding to the minimum value of the objective function to calculate the values of other remaining variables σ_1, σ_3, and L_2 and further solve the coordinates of each reflector at the center point and the parabolic main reflector at the vertex according to the simultaneous equations and the geometric structure of the CATR system. To demonstrate the effectiveness of the proposed universal applicability design method, here we use this strategy to create four tri-reflector CATRs corresponding to four different feed rotation angles, respectively, by using this approach. Table 2 lists the values of the corresponding key parameters when the angle θ_0 is at 0°, 30°, 60°, and 90°, respectively.

Next, we use the dynamic ray-tracing method to shape the two subreflectors. First, according to the law of conservation of energy, we establish a mapping function $(x, y) = F(\theta, \varphi)$ between the beam with the output direction (θ, φ) emitted from the feed and the position (x, y) where the beam finally reaches the output field so that the beam energy emitted from the feed is redistributed according to the required field on the aperture plane.

Second, we divide the feed beam into multiple subbeams (i.e., optical paths) according to dynamic beam tracing and calculate the specular parameters of the shaped subreflectors on the central optical path according to the optical center points of each mirror determined previously. By using the principle of the intersection of the central optical path and

Table 2: The variable values of the corresponding tri-reflector CATR for four different feed rotation angles.

Parameters	α (°)	σ_1 (°)	σ_2 (°)	σ_3 (°)	L_0 (m)	L_1 (m)	L_2 (m)	R_3 (m)
$\theta_0 = 0°$	25	25	60.1	35.1	0.6	0.97	4.73	5.39
$\theta_0 = 30°$	−9.5	25.1	36	45.5	0.6	1.2	3.55	3.3
$\theta_0 = 60°$	−16.7	43.6	46.8	63.5	0.6	1.0	3.58	3.3
$\theta_0 = 90°$	−20.3	69.7	68.1	88.4	0.6	0.9	3.25	3.0

the double parabolic expansion surface, the position of the new reflection points on the shaped subreflectors can be calculated, and then the new specular parameters of the shaped mirrors on the new optical path can be obtained by using the dynamic ray-tracing method. We repeat the previous steps in the loop, extend the design from the specular optical center to the edge, and successively obtain the position of the reflection point on the shaped subreflector on the next optical path, until the specular parameters of the shaped subreflector on the last optical path are obtained. Here, the solution method for the position of the new reflection point is shown in Figure 3. Taking the first shaped subreflector as an example, first, a new beam is emitted from the feed, which has a new output direction, assuming that the position of the new beam reflection point is $\mathbf{r}_{\text{new}}$, then we get the following equation:

$$\mathbf{r}_{\text{new}} = \mathbf{r}_{\text{feed}} + s\hat{s}, \tag{3}$$

where $\mathbf{r}_{\text{feed}}$ represents the position of the feed and s and $\hat{s}$ are the distance from the new reflection point to the feed and the new beam propagation vector, respectively. Moreover, the position $\mathbf{r}_{\text{new}}$ of the new reflection point on the double-parabolic expansion surface of the known optical center point is as follows:

$$\mathbf{r}_{\text{new}}(x, y) = \mathbf{r}_{\text{known}} + x\hat{g}_1 + y\hat{g}_2 - \frac{1}{2}\left(x^2 G_1 + y^2 G_2\right)\hat{n}, \tag{4}$$

where $\mathbf{r}_{\text{known}}$ is the known optical center position, $\hat{n}$ is the propagation unit vector, $\hat{g}_1$ and $\hat{g}_2$ are the two mutually perpendicular principal curvature vectors of the wavefront surface at the known optical center point, G_1 and G_2 are the corresponding curvatures, and x and y are two unknown variables. By combining formulas (3) and (4) to calculate the unknown variables x, y, and s, then the position of the new reflection point can be obtained.

Finally, according to the obtained specular parameters at all reflection points, the surfaces of the two shaped subreflectors can be determined numerically.

Furthermore, the realization principle of the kinematic and dynamic ray-tracing method is programmed in MATLAB numerical analysis software, and the values of all key parameters and coordinate points obtained above are substituted into the written program to carry out the numerical calculation. In this way, we can obtain the two shaped subreflectors, which are composed of discrete data points.

In order to verify the effectiveness of the proposed design method, the designed tri-reflector CATR is numerically simulated in commercial simulation software GRASP-10. The specific simulation process is as follows: firstly, we bring the obtained surface data on the shaped mirrors into the reflector class attribute of GRASP to model the subreflectors, and we set the calculated relevant parameter values in software. Secondly, we use an ultra-Gaussian corrugated horn as the feed, which has a pattern taper of −21.6 dB at 18°, and its sidelobe level and cross-polarization are less than −36 dB and −45 dB, respectively, as shown in Figure 4. Finally, we use the physical optics (PO) plus physical theory of the diffraction (PTD) calculation method to calculate the surface current, which is generated by the feed illuminating subreflector1, subreflector2, and the main reflector in sequence, and then we obtain the QZ performance of the output field.

To further verify the universal applicability of the design method to any feed rotation angle, according to the above simulation process, four tri-reflector CATRs corresponding to four different feed rotation angles have been modeled and simulated, respectively, by GRASP-10, as shown in Figure 5.

3. Results and Discussion

In the design of a tri-reflector CATR system, three important characteristics need to be considered, and they are phase ripple, amplitude ripple, and cross-polarization. The phase ripple in major is determined by the optical path, while the amplitude ripple is subjected to the ability of a system to tailor the energy distribution. Moreover, cross-polarization mainly depends on the geometric configuration of the system and the relative positions of the reflectors. For the realization of low cross-polarization, we adopted the beam mode analysis and cross-polarization elimination condition method in Section 2.1, and for reducing the amplitude and phase ripple, we followed the method of the dynamic ray-tracing method. These are the keys to designing the tri-reflector CATR.

Since CATR is primarily utilized for high-frequency antenna measurement, the ultra-Gaussian corrugated horn with Gaussian far-field distribution is used as the feed in our design. For the system's aperture field distribution, the "Uniform + Gaussian" distribution is adopted as an objective function. Moreover, the edge illumination on the output aperture is −24 dB; meanwhile, the diameter of the output QZ field is designed to be 2.1 m. Such a distribution is uniform over a large range of the aperture but quickly attenuates towards the edge, which can effectively reduce the influence of edge diffraction to a certain extent. According to the simulation process in Section 2.2, for the designed four tri-reflector CATRs corresponding to four different feed rotation angles, the simulated QZ results of the output field on the principal cuts at 100 GHz, 300 GHz, and 500 GHz are illustrated in Figures 6–8, respectively, which are summarized in Table 3.

It is worth noting that if the effects of transmission loss and edge diffraction are not considered, the copolar amplitude of the aperture field obtained by the reflection of the parabolic reflector is a constant in theory, and at the same time, the optical paths of all rays transmitted from the feed to the aperture surface of the QZ are equal, so the QZ field

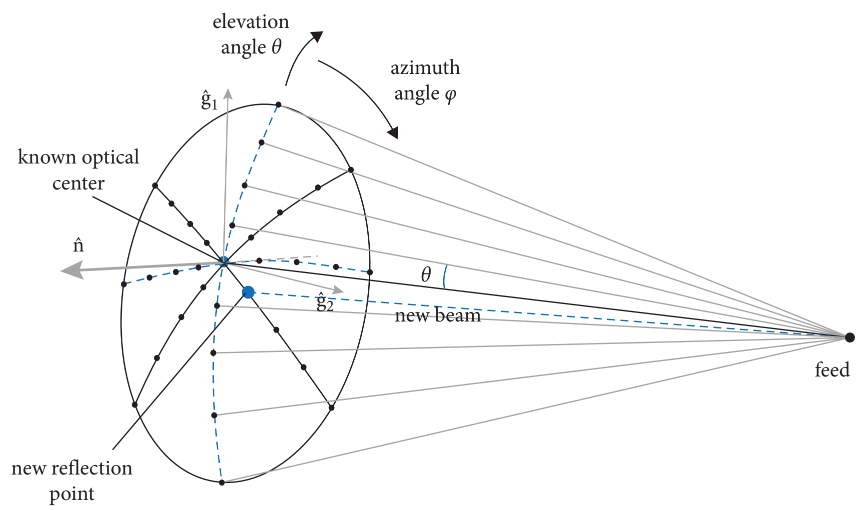

FIGURE 3: The solution of the new reflection point of the shaped subreflector based on the intersection of the double parabolic expansion surfaces.

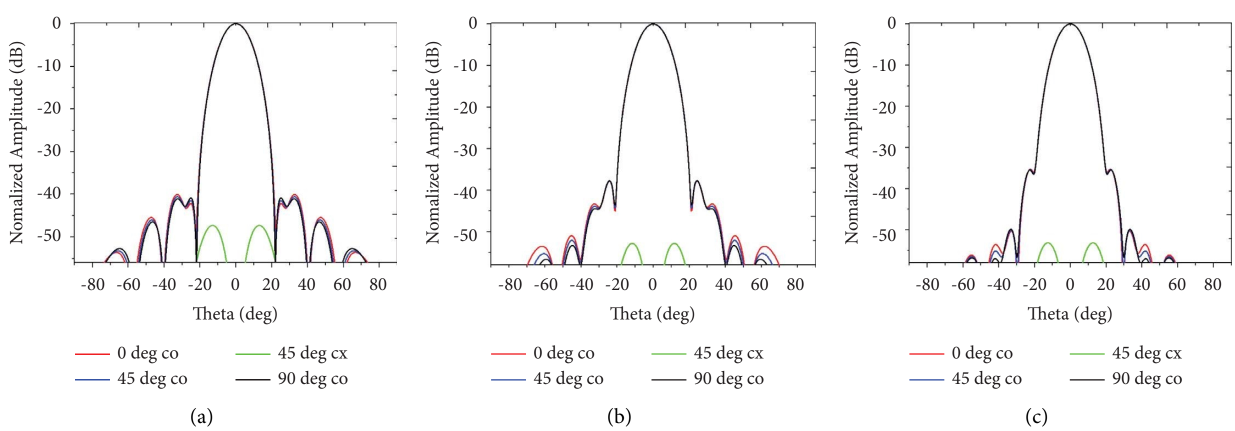

FIGURE 4: Ultra-Gaussian corrugated horn feed radiation pattern. (a) 100 GHz, (b) 300 GHz, and (c) 500 GHz.

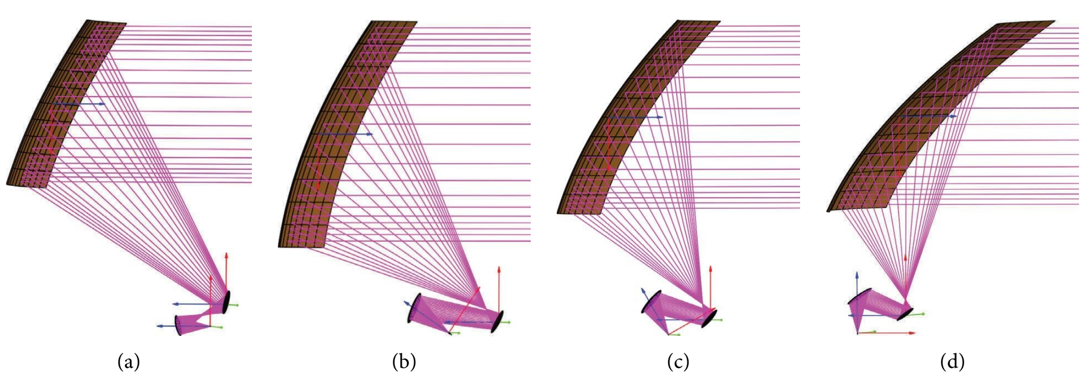

FIGURE 5: Four tri-reflector CATRs corresponding to different geometric configuration forms for different feed rotation angles. (a) $\theta_0 = 0^\circ$. (b) $\theta_0 = 30^\circ$. (c) $\theta_0 = 60^\circ$. (d) $\theta_0 = 90^\circ$.

theoretically has an even copolar amplitude and phase distribution, which are shown by the black solid line in Figures 6–8, and these distribution curves can be used as the objective copolarization amplitude and phase curves that we need to get. In the synthesis by the ray-tracing process, because the objective function of the output field is adopted a "Uniform + Gaussian" aperture field distribution, so the copolar amplitude taper in the designed quiet zone is 0 dB.

From the simulation results in Figures 6–8, it can be seen that when the rotation angle of the feed is at 0°, 30°, 60°, and

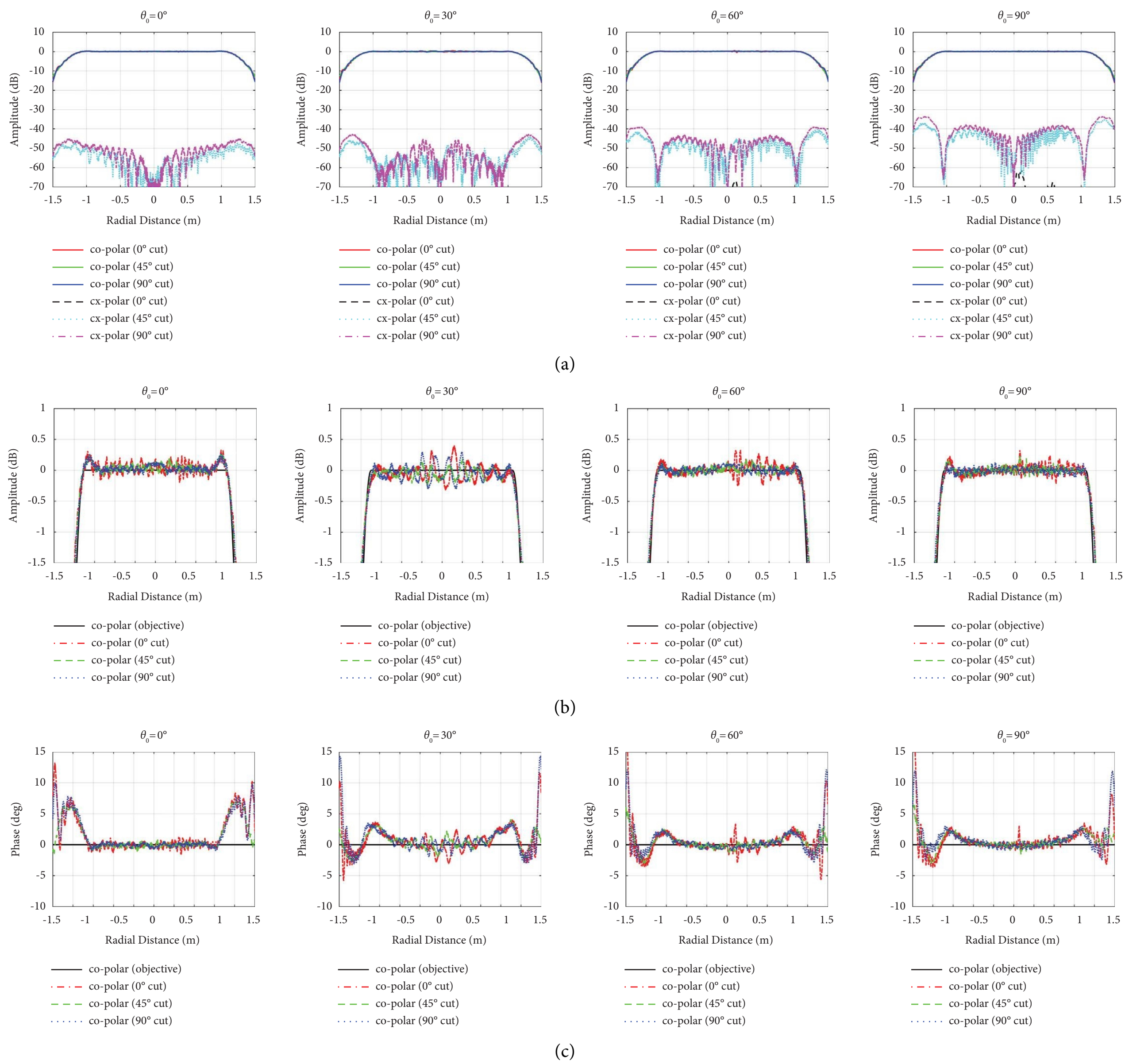

Figure 6: PO + PTD one-dimensional normalized simulation results of the designed tri-reflector CATRs with different feed rotation angles at 100 GHz. (a) Cross-polar isolation, (b) copolar amplitude, and (c) copolar phase.

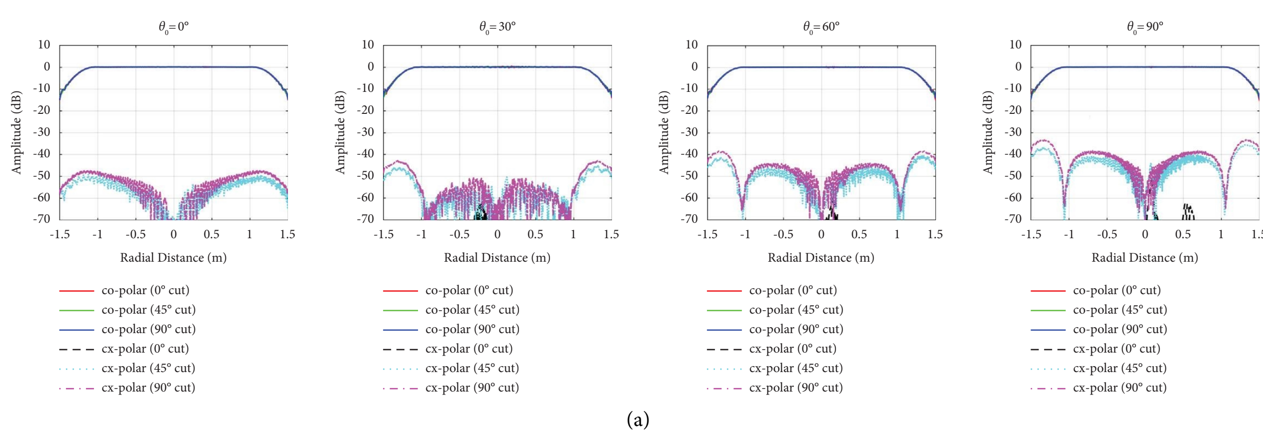

Figure 7: Continued.

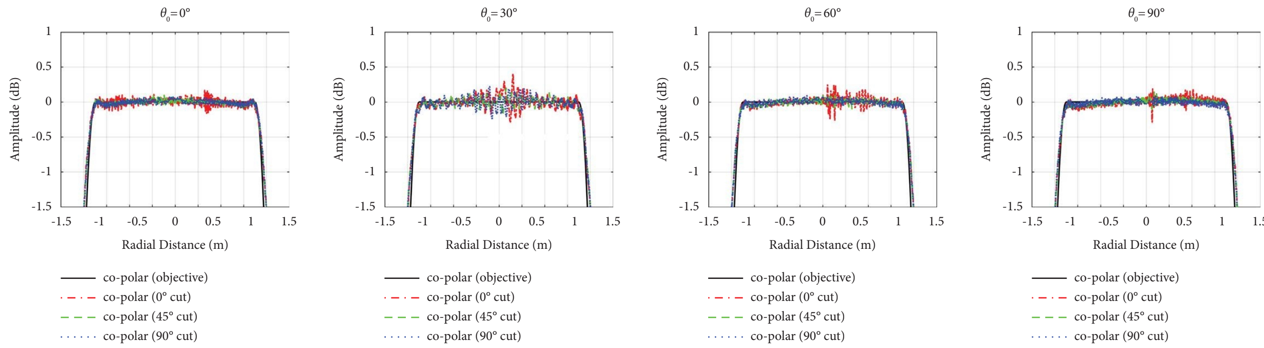

(b)

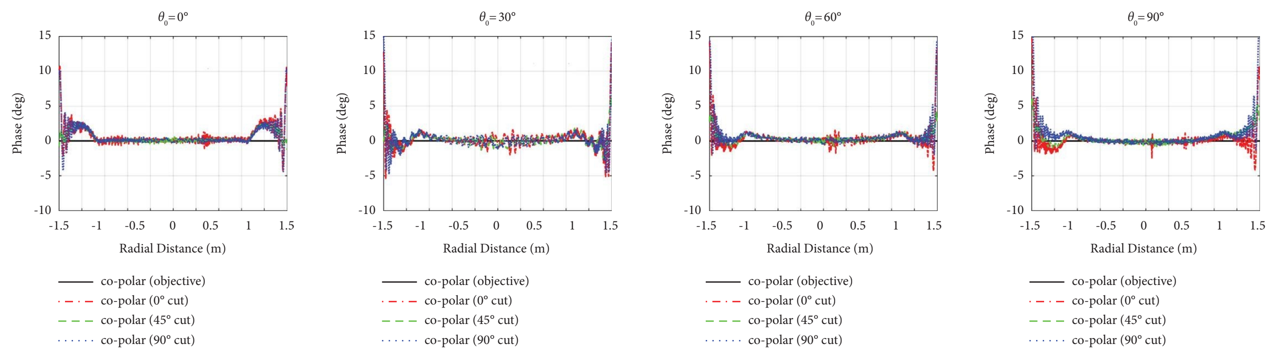

(c)

Figure 7: PO + PTD one-dimensional normalized simulation results of the designed tri-reflector CATRs with different feed rotation angles at 300 GHz. (a) Cross-polar isolation, (b) copolar amplitude, and (c) copolar phase.

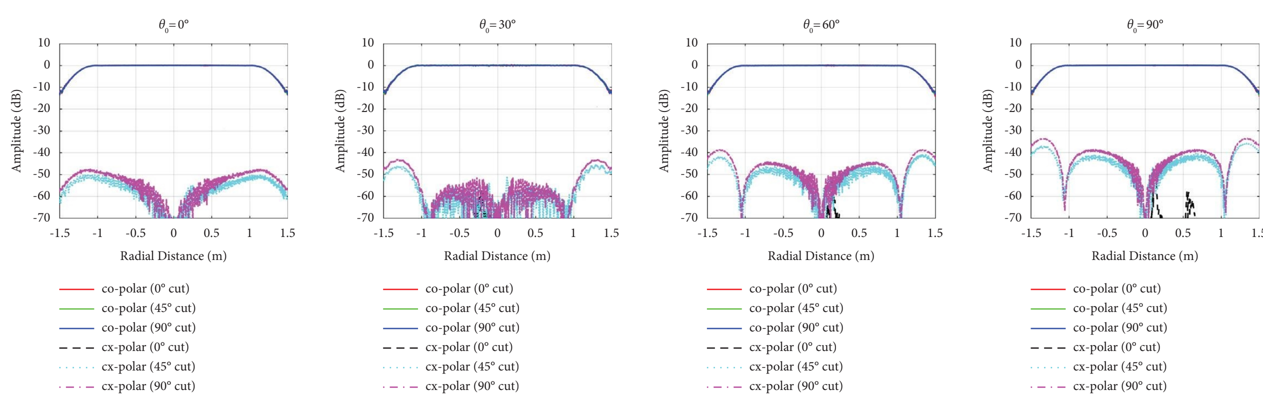

(a)

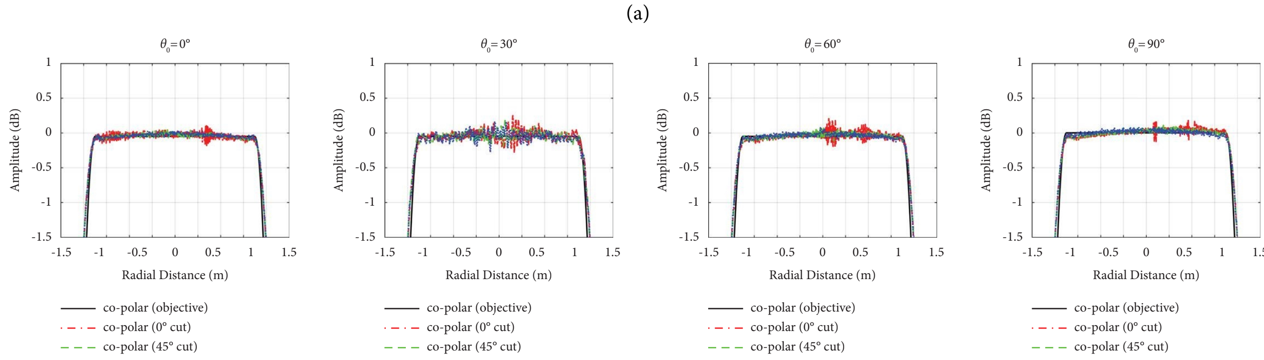

(b)

Figure 8: Continued.

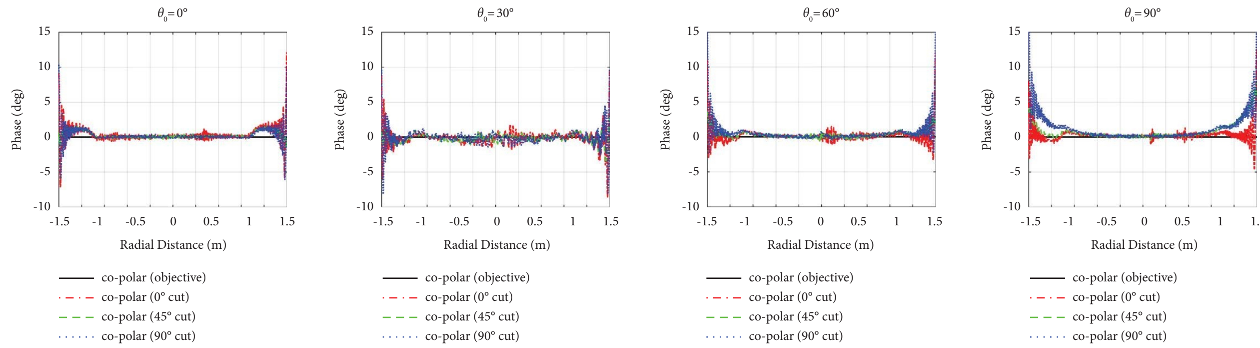

(c)

Figure 8: PO + PTD one-dimensional normalized simulation results of the designed tri-reflector CATRs with different feed rotation angles at 500 GHz. (a) Cross-polar isolation, (b) copolar amplitude, and (c) copolar phase.

Table 3: Quiet zone performance of the four designed tri-reflector CATRs corresponding to four different feed rotation angles (the QZ usage is 70%).

Feed rotation angles (°)	Frequency (GHz)	Copolar amplitude ripple (dB)	Copolar phase ripple (°)	Cross-polar (dB)
0	100	0.52	4.42	−47.59
	200	0.39	3.12	−47.71
	300	0.33	2.81	−47.58
	400	0.35	2.07	−47.48
	500	0.27	1.83	−47.67
30	100	0.69	6.86	−45.94
	200	0.68	4.45	−47.84
	300	0.63	3.78	−49.39
	400	0.54	3.65	−50.94
	500	0.48	3.69	−50.54
60	100	0.63	5.71	−42.48
	200	0.54	3.82	−43.21
	300	0.47	3.39	−43.35
	400	0.39	2.97	−43.37
	500	0.36	2.77	−43.79
90	100	0.54	5.12	−37.83
	200	0.52	4.37	−38.34
	300	0.47	4.03	−38.48
	400	0.39	3.68	−38.37
	500	0.31	2.78	−38.71

90°, respectively, the maximum value of cross-polarization is −37.83 dB, and the maximum value of copolar amplitude (phase) ripples is 0.69 dB (6.86°) for the designed four tri-reflector CATRs in the designed working frequency range. Due to the effects of reflector edge diffraction, feed spillover, and multiple reflections of stray fields, there are some chaotic ripples in the center area of the simulated QZ, especially at low frequencies, but the copolar amplitude and phase curves of the simulated CATR are still relatively flat in general. Moreover, all of these simulation results are within the QZ evaluation criteria of cross-polarization <−30 dB and peak-to-peak amplitude (phase) ripple < 1 dB (10°) required by the standard CATR. It can also be seen from the figures that the QZ diameter of the copolar amplitude and phase in the center area is about 2.1 m; that is, it achieves a high QZ usage of up to 70%, which demonstrates that the designed CATRs have good QZ performance.

Finally, Table 3 lists the specific data of the simulated QZ performance of the designed four tri-reflector CATRs corresponding to four different feed rotation angles, respectively. It can be seen that all the designed tri-reflector CATRs cover a wider frequency range from 100 GHz to 500 GHz. Because of the edge diffraction effect of the reflector surface, the copolar amplitude and phase have higher ripples at low frequencies, but as the simulation frequencies increase, the ripples gradually decrease, and the quiet zone performance is also gradually improved. For all of these tri-reflector CATRs in different feed rotation angles, the cross-polarization of the tri-reflector CATR corresponding to 0° feed rotation angle is relatively lower, which illustrates that the geometric structure of the system and the relative position of each reflector have an important influence on the cross-polarization of the tri-reflector CATR. So far, the feasibility and effectiveness of the proposed universal applicability design method for the design of low cross-polarization tri-reflector CATR have been theoretically implemented, and the obtained QZ performance is in good agreement with the theoretical analysis.

4. Conclusions

In this paper, a novel universal applicability design method and procedure with low cross-polarization characteristics for the design of terahertz tri-reflector CATR is proposed and has been theoretically implemented. According to beam mode analysis and cross-polarization elimination theory and the dynamic ray-tracing method, four low cross-polarization tri-reflector CATRs with different feed rotation angles are synthesized. Numerical simulation results show that no matter whether the rotation angle of the feed is at 0°, 30°, 60°, or 90°, the cross-polarization of the designed four tri-reflector CATRs are all less than −38 dB, and the peak-to-peak amplitude (phase) ripples of four tri-reflector CATRs are all within 1 dB (10°) on the principal cuts of the designed QZ at 100–500 GHz. Furthermore, the QZ usage ratios of these tri-reflector CATRs are all better than 70%. All these clearly demonstrate the feasibility and effectiveness of the universal applicability theoretical design method. The method not only greatly improves the flexibility of feed installation position and space usage in a CATR system, but it also has universal applicability to the design of a tri-reflector CATR with low cross-polarization characteristics in any different feed rotation angles. This provides crucial conditions for us to reasonably layout and construct the entire tri-reflector CATR system as well as flexibly design and install various forms of feed in the case of limited space size in the actual environment so as to realize the CATR with higher performance, which has important research prospects and engineering application value.

Data Availability

The data used to support the findings of this study are included within the article.

Conflicts of Interest

The authors declare that they have no conflicts of interest.

Acknowledgments

This work was supported by the Fundamental Research Funds for the Central Universities (BUPT Project No.: 2021XD-A08-2).

References

[1] P. de Maagt, "Terahertz technology for space and earth applications," in *Proceedings of the 2006 First European Conference on Antennas and Propagation*, pp. 1–4, Nice, France, November 2006.

[2] A. J. Nozik, "Spectroscopy and hot electron relaxation dynamics in semiconductor quantum wells and quantum dots," *Annual Review of Physical Chemistry*, vol. 52, no. 52, pp. 193–231, 2001.

[3] T. Sarkar and A. Taaghol, "Near-field to near/far-field transformation for arbitrary near-field geometry utilizing an equivalent electric current and MoM," *IEEE Transactions on Antennas and Propagation*, vol. 47, no. 3, pp. 566–573, 1999.

[4] A. Yaghjian, "An overview of near-field antenna measurements," *IEEE Transactions on Antennas and Propagation*, vol. 34, no. 1, pp. 30–45, 1986.

[5] M. Jin, B. Fan, D. Xia, and B. Ming, "Application of the FFT-PVVA fast solution in designing terahertz compact antenna test range," in *Proceedings of the International Applied Computational Electromagnetics Society Symposium-China (ACES)*, pp. 2-3, Nanjing, China, August 2019.

[6] X. Liu, Y. Mai, H. Su et al., "Design of tri-reflector Compact Antenna Test Range for millimetre/sub-millimetre wave and THz antenna measurement," in *Proceedings of the 2011 International Workshop on Antenna Technology (iWAT)*, pp. 144–147, Hong Kong, China, March 2011.

[7] C. Rieckmann, M. R. Rayner, and C. G. Parini, "Optimisation of cross-polarisation performance for tri-reflector CATR with spherical main reflector," *Electronics Letters*, vol. 35, no. 17, pp. 1403-1404, 1999.

[8] I. J. Gupta, D. G. Brown, W. D. Burnside, and W. Lin, "A serrated edge gregorian subreflector for dual chamber compact range systems," *IEEE Transactions on Antennas and Propagation*, vol. 39, no. 8, pp. 1258–1261, 1991.

[9] C. Rowell, A. Cardalda-Garcia, and B. Derat, "CATR reflector measurement system with multiple reflectors for multiple angles of arrival in millimeter-wave frequency bands," in *Proceedings of the Antenna Measurement Techniques Association Symposium (AMTA)*, pp. 1–6, Newport, RI, USA, November 2020.

[10] A. Karttunen, J. Ala-Laurinaho, M. Vaaja et al., "Antenna tests with a hologram-based CATR at 650 GHz," *IEEE Transactions on Antennas and Propagation*, vol. 57, no. 3, pp. 711–720, 2009.

[11] B. S. Westcott, F. Brickell, and I. C. Wolton, "Crosspolar control in far-field synthesis of dual offset reflectors," *IEE Proceedings H - Microwaves Antennas and Propagation*, vol. 137, no. 1, pp. 31–38, 1990.

[12] C. Parini, C. Rieckmann, and R. Donnan, "Experimental validation of the design performance for a spherical main mirror tri-reflector CATR operating at 90 GHz," in *Proceedings of the 28th ESA Antenna Workshop on Space Antenna Systems and Technologies*, vol. 1, pp. 393–400, Noordwijk, Netherlands, 2005.

[13] K. Aoki, S. Makino, M. Masuda, and S. Urasaki, "A design method of an offset tri-reflector antenna whose main reflector is of an offset parabola type with high efficiency and low cross-polarization characteristics," *Electronics and Communications in Japan*, vol. 83, no. 10, pp. 72–82, 2000.

[14] C. G. Parini, A. D. Olver, P. Mcnair, and C. J. Prior, "The design, construction and use of a millimeter wave compact antenna test range," in *Proceedings of the 1989 Sixth International Conference on Antennas and Propagation, ICAP*, vol. 89, pp. 345–350, Coventry, UK, April 1989.

[15] A. Muñoz-Acevedo, S. Burgos, and M. Sierra-Castañer, "Performance comparison between serrated edge and rolled edge reflectors inside CATR facilities," in *Proceedings of the 5th European Conference on Antennas and Propagation (EUCAP)*, pp. 3586–3590, Rome, Italy, April 2011.

[16] L. Le Coq, B. Fuchs, T. Kozan, T. Andersson, and S. Burgos, "Compact antenna test range implementation in IETR millimetre wave antenna test facility," in *Proceedings of the IEEE Conference on Antenna Measurements & Applications (CAMA)*, pp. 1–4, Antibes Juan-les-Pins, France, November 2014.

[17] R. Liu, I. Lin, and J. Liang, "A new compact test range for satellite antenna measurements," in *Proceedings of the*

International Symposium on Antennas and Propagation Conference Proceedings, pp. 1-2, Kaohsiung, Taiwan, 2014.

[18] J. P. McKay and Y. Rahmat-Samii, "An array feed approach to compact range reflector design," *IEEE Transactions on Antennas and Propagation*, vol. 41, no. 4, pp. 448–457, 1993.

[19] J. P. McKay and Y. Rahmat-Samii, "Multi-ring planar array feeds for reducing diffraction effects in the compact range," *AMTA Proceedings*, pp. 3–8, Columbus, America, 1992.

[20] R. Jana and R. Bhattacharjee, "A tri-mode low cross-polarized circular matched feed for offset reflector antenna system," in *Proceedings of the 20th First National Conference on Communications (NCC)*, pp. 1–6, Mumbai, India, February 2015.

[21] E. Lier and S. A. Skyttemyr, "A shaped single reflector offset antenna with low cross-polarization fed by a lens horn," *IEEE Transactions on Antennas and Propagation*, vol. 42, no. 4, pp. 478–483, 1994.

[22] R. A. Nair and R. Shafiei, "A multimode pyramidal horn with symmetrical dielectric loading-a high efficiency feed for reflector antennas in satellite communications," in *Proceedings of the International Symposium on Antennas and Propagation Society*, pp. 1522–1525, Dallas, TX, USA, May 1990.

[23] J. Hartmann and D. Fasold, "Analysis and performance verification of advanced compensated compact ranges," in *Proceedings of the 29th European Microwave Conference*, pp. 146–149, Munich, Germany, October 1999.

[24] C. H. Schmidt, H. J. Steiner, S. Klett, H. Garcia, and G. Forma, "Quiet zone extension of an existing compensated compact range 75/60," in *Proceedings of the 2015 9th European Conference on Antennas and Propagation (EuCAP)*, pp. 1–5, Lisbon, Portugal, April 2015.

[25] C. Yang, J. Yu, Y. Yao, X. Liu, and X. Chen, "Numerical synthesis of tri-reflector CATR with high cross-polarisation isolation," *Electronics Letters*, vol. 52, no. 15, pp. 1286–1288, 2016.

[26] S. G. Hay, "Ray-transformation conditions and shaped-reflector solutions for three-reflector optics without cross-polarization," *IEEE Transactions on Antennas and Propagation*, vol. 55, no. 8, pp. 2174–2184, 2007.

[27] T. Furuno, S. Urasaki, and T. Katagi, "Tri-reflector antennas eliminating cross-polarized component based on beam-mode analysis," *Electronics and Communications in Japan*, vol. 79, no. 7, pp. 55–64, 1996.

[28] T. Furuno, S. Urasaki, T. Katagi, and H. Ikuno, "Multireflector offset antennas eliminating cross-polarization component based on beam mode analysis," *Electronics and Communications in Japan*, vol. 84, no. 12, pp. 1–12, 2001.

[29] P. S. Kildal, "Analysis of numerically specified multireflector antennas by kinematic and dynamic ray tracing," *IEEE Transactions on Antennas and Propagation*, vol. 38, no. 10, pp. 1600–1606, 1990.